CESARE'17
COORDINATING ENGINEERING FOR SUSTAINABILITY AND RESILIENCE
Dead Sea, Amman, Jordan
3-8 May 2017
JORDAN UNIVERSITY OF SCIENCE & TECHNOLOGY
IRBID - JORDAN

NUMERICAL INVESTIGATION OF THE ENHANCED PERFORMANCE OF SOLAR PONDS USING NANOPARTICLES

Argyrios Anagnostopoulos

School of Chemical Engineering
University of Birmingham
Birmingham, B15 TK1, United Kingdom
e-mail: axa1217@student.bham.ac.uk;

Keywords: Solar pond, Nanoparticle, Numerical Modelling, Thermal Enhancement, Sustainability

Abstract: *A series of numerical models was developed in order to predict and investigate the thermal performance of a Salinity Gradient Solar Pond (SGSP). A 1-D simplified model using non-linear first order differential equations was developed in MATLAB and a more elaborated 2D and 3D finite element model was developed in COMSOL Multiphysics, based on a set of Partial Differential Equations, which govern the phenomena of heat transfer and radiation in semi-transparent media. The developed models were validated in terms of their accordance with published experimental data sets from two different test sites. The potential enhancement of the thermal performance of a SGSP by adding nanoparticles in the Lower Convective Zone (LCZ) was investigated numerically. The existence of the nanoparticles was simulated taking into account their thermal and optical properties. The 3D model showed an average temperature increase of 9.8* ^{o}C *in its LCZ, whereas the 2D presented a temperature increase of 5.9*^{o}C*. The 1D model showed the least improvement (4.9* ^{o}C*). This was attributed to the ability of the 2D and 3D models to account for the optical properties of the suspended nanoparticles. In all cases the thermal enhancement contributed by the nanoparticles is evidently positive.*

1 INTRODUCTION

Solar thermal applications are the best alternative among the renewable energy technologies in an economic point of view [1]. A popular device is a solar pond. Solar ponds have applications in industrial heat process, agriculture, electrical power generation, chemical productions, desalination, refrigeration and air conditioning and swimming pool heating [2],[3].

A solar pond is a pond filled with saline water consisting of 3 zones. The first zone is the Upper Convecting Zone (UCZ), which is the smallest of the 3 zones. It has a height of 0.1 to 0.3m. It consists entirely of pure water. The second is the Non Convective Zone (NCZ), which is the middle zone of the solar pond. It has a downward increasing salinity profile and is not homogenous. The final one is the Lower Convection or Heat Storage Zone (LCZ/HSZ), which consists of brine with the maximum degree of salt solubility and depending on the type of salt has a salinity of 20 to 26%. In all of its applications the heat is either provided directly through the extraction of the hot brine or with the use of a network of heat exchangers in the bottom and side wall areas of the solar pond.

A solar pond has the ability to minimize heat loss by convection, through its density-gradient created with the help of high salinity water. The concentrations are very low at the surface of the pond and at maximum solubility at its bottom. This design is called the salinity gradient solar pond. A major part of the pond going downwards is infused with a salt gradient to establish its stability against upward fluid movement. Therefore, the only type of upward heat loss from bottom to top is conduction. This mechanism works against the density reduction that occurs due to the increase of temperature, due to the absorbed solar radiation at the ponds lower part. Furthermore, the thermal conductivity of the salt, which is lesser than that of pure water, decreases with increasing salinity and thus acts as multiple layers of insulation enhancing the storage phenomena even more, as it also increases the boiling point of water [4].

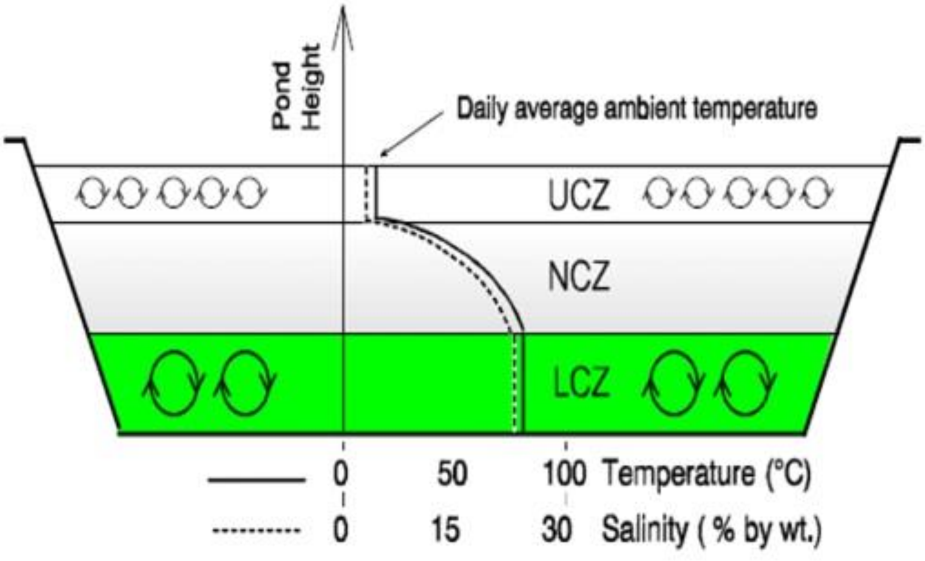

Figure 1: A Salinity Gradient Solar pond [5]

A trending research topic in the last decade is the addition of nanoparticles (NPs) in fluids in order to enhance the performance of the base fluid. It has been shown that the addition of NPs has a considerable impact on the base fluid's thermophysical properties such as the thermal conductivity [6], mass diffusivity [7] and viscosity [8]. In solar thermal applications nanoparticles have shown to increase efficiency for solar collectors by a generous bit with very small concentration of below 0.1% [9]. In the same mindset, they could be also be implemented in the LCZ of a solar pond in order to enhance its performance. Research in that area is still limited.

Karunamurthy et al. [7] investigated the use of nanoparticles in enhancing the heat transfer efficiency from a SGSP to a Low Energy Storage System using nanoparticles. They constructed a very small scale (50x50x25cm) model of a SGSP and heated it by a heater. The hot saline water was pumped to a storage that contained a phase change material (paraffin) mixed with nanoparticles (CuO).

Al-Nimr et al. [10], developed a numerical model to simulate the impact of adding Ag NPs on the performance of a shallow solar pond (SSP). In his model the pond's lower layer is assumed to be a uniformly mixed Ag-nanofluid and the pond's upper layer paraffin. The results of the model showed that the energy stored in the nanofluid pond is more than twice of that of the brine pond. Due to the enhanced optical properties the solar absorption was increased and due to the thermal properties a reduction of heat losses was also observed.

Hamdan et al. [11], also investigated the addition of nanoparticles in a shallow solar pond. In their work two shallow solar ponds were constructed and installed side by side to study the effect of adding aluminum oxide AL2O3 nanoparticles (one with nanoparticles , while the other one without). It was found that the performance of the shallow solar pond in general was improved with an increase in the temperature of the lower convective zone varies between 2.1oC to 11.3oC, with the maximum increase is obtained when 0.2% concentration of nanoparticles.

Both the works of Al-Nimr and Hamdan were conducted in SSPs. SSPs are small tanks with a depth of a few centimeters and a small surface area fitting for domestic scale applications. They are also sealed on the top with a plastic or glass cover. Therefore, although they work in a similar way in terms of absorbing sunlight the storage principle is different. Consequently, no experimental or theoretical work has been yet conducted in terms of adding nanoparticles in SGSPs.

It is evident that a gap exists in research in SGSPs related to the potential enhancement of their performance through the addition of NPs in the LCZ (Anagnostopoulos, 2016)[12].

2. SIMULATION OF THE PROBLEM

2.1 Introduction

In the present study two models were developed in order to investigate the possible enhancement that nanoparticles can provide to the performance of an SGSP. A 1D mode was developed, using MATLABR2013 [13] and a 2D/3D model using COMSOL Multiphysics [14].

Firstly a simplified methodology, developed by Sayer [15] and based on an one dimensional analysis using non-linear first order differential equations of the conservation of energy of the UCZ and LCZ, was implemented in a computer code using MATLABR2013 [13]. This method was able to account for the nanoparticles only in terms of specific heat capacity and density.

The second methodology, was developed using COMSOL Multiphysics, a finite element software. According to the proposed methodology firstly the geometry of the pond and the zones are simulated and then sets of Partial Differential Equations that best govern the phenomena and the behavior of the material are selected from an extended library. For certain phenomena such as the heat loss by Evaporation or the heat loss from the side walls of the pond, empirical supplementary equations are applied. In this study the "Heat Transfer with Radiation in Participating Media" module of COMSOL was used to calculate temperature distribution in the solar pond. This module combines features from the "Radiation in Participating Media" and "Heat Transfer" module. This enables the modeling of radiative heat transfer inside a participating medium. This module solves for radiation intensity field as well as heat transfer between the solids and fluids included in the geometry.

2.2 2D/3D Simulation

In order to model the performance of a SGSP the temperature of the LCZ must be accurately predicted. The governing phenomena for the temperature variation in the LCZ are the incident intensity that penetrates the surface of the pond as well as heat transfer due to convection and conduction. Therefore two governing equations were applied one to model the incident intensity and one the heat transfer. They were accompanied by several supplementary equations as well as some semi-empirical formulas used in the boundaries of the solar pond geometry (see below).

The equation that describes the behavior sunlight propagated in a semi-transparent media such as water is [14]:

$$\Omega_i * I_i = \kappa * I_b(T) - \beta * I_i + \frac{\sigma_s}{4\pi} * \int_0^{4\pi} \omega_j I_j * \varphi(\Omega_j, \Omega_i) \quad (1)$$

where, $I_b(T)$ blackbody radiation intensity (W/m^2), $I_{i,j}$ the radiation Intensity in different directions (W/m^2), T the temperature (°C), κ the absorption coefficient (1/m), β the extinction coefficient (1/m), σ the scattering coefficient (1/m), n the refractive Index, Φ the scattering phase function and Ω direction of the radiative intensity.

In order to couple radiation in participating media with heat transfer, radiative heat flux is taken into account in addition to conductive heat flux and the heat transfer equation takes the following form [14]:

$$\rho * C_p * \left(\frac{\partial T}{\partial t}\right) = -\nabla * q_c + Q_r + Q \quad (2)$$

where, ρ the density (kg/m^3), C_p the specific heat capacity at constant pressure (J/(kg*K), T the temperature (°C), Q_r the radiative heat source (W/m^3), q_c the conductive heat flux (W/m^2) and Q work related heat flux (W/m^2).

2.3 Boundary Conditions

Incident Intensity

In order to model the radiation input for the solar pond an incident intensity on the boundary representing the surface of the solar pond was specfied. In order to simulate the model in a yearly basis an interpolation function was set as input for the variable of the incident intensity. However, it is known that the total power of a transmitted wave is not the actual incident wave that reaches a surface. The transmission coefficient τ is a value that is used to describe the relation between transmitted wave and the final incident wave, its essentialy a ratio of the part of the transmitted wave that reaches a surface. Therefore, the iraddiance values were modified according to Wang [16]to account for the refelection values and incident angle with a τ=0.85.

Evaporative Heat Loss

In order to compute the daily evaporative heat loss from the surface of the pond a small script was coded using MATLAB. A semi-empirical formula was used in this research is from the work of Hull [17], as it accounts for several parameters including the vapor pressure of water, the partial pressure of water, the wind speed and the relative humidity.

Side Heat Losses
In order to account for losses from the side walls a heat convection (Q_{con}) equation was applied in the side wall boundaries of the pond, which has the following format [14]:

$$Q_{con} = h * (T_{ext} - T) \tag{3}$$

Where, h was replaced with the value of the inverse of the thermal resistance, in order to account for the thickness and type of insulation. T_{ext} the ambient Temperature (°C) and T the temperature of the boundary (°C).

Bottom Heat Losses
In order to account for losses from the bottom of the pond a second heat flux was introduced. With the same format as in equation (3). However this time the heat transfer coefficient for heat loss to the ground was calculated according to Hull [18].

Radiation Heat Loss
In order to account for radiation heat losses the general equation for surface to ambient radiation (Q_{rad}) was applied. It has the following format:

$$Q_{rad} = \varepsilon * \sigma * (T_{amb}^4 - T^4) \tag{4}$$

A surface emissivity of ε=0.83 was chosen and the external temperature (T_{amb}) was replaced by an interpolation function containing the yearly daily sky temperature data calculated using the formula provided by Swinbank [19].

2.4 System Properties

A set of empirical formulas were used to determine the required thermophysical properties of water. The density and specific heat capacity of water were calculated with respect to salinity, while the thermal conductivity with respect to salinity and temperature. The maximum temperature recorded in a SGSP was 103°C [18] and the maximum salt concentration in water is 26% for NaCl at 100°C. The minimum temperature levels are close to 0°C in winter months and for salinity 0% at the UCZ of the solar pond.

The thermophysical parameters present in eq 4 are the density which was computed according to Jamal [20], the specific heat capacity that was measured using the formula provided by Kleinstreuer [21] and the thermal conductivity calculated by the equation provided by Al-Nimr [10].

The required optical properties are the absorption coefficient, the scattering coefficient and the refractive index. Since, it was assumed that there is a constant pressure, the main properties that change within the solar pond are the temperature and the salinity. Therefore the dependence of the 3 optical properties (absorption scattering and refractive index), that are used in the selected physics, on salinity and temperature was identified. The base values of the properties in the case of water were provided by Bukata [22]. Rottgers provides information related to the dependence of absorption and scattering coefficients as well as the refractive index on temperature and salinity [23, 24].

2.5 Validation of the two models

The three models described above were validated using existing experimental data sets provided by solar pond operations in different countries. In Figure 2 the temperature of the LCZ of the solar pond is shown for all 3 models in comparison with the experimental data found in the work of Ali concerning a 4x2x0.5m SGSP located in Kuwait City, Kuwait [25]. The input meteorological data were taken from NASA.

From Figure 2 it can be seen that all 3 models present a very good agreement with the experimental data sets. Evident is also the higher accuracy provided by the 3-D model.

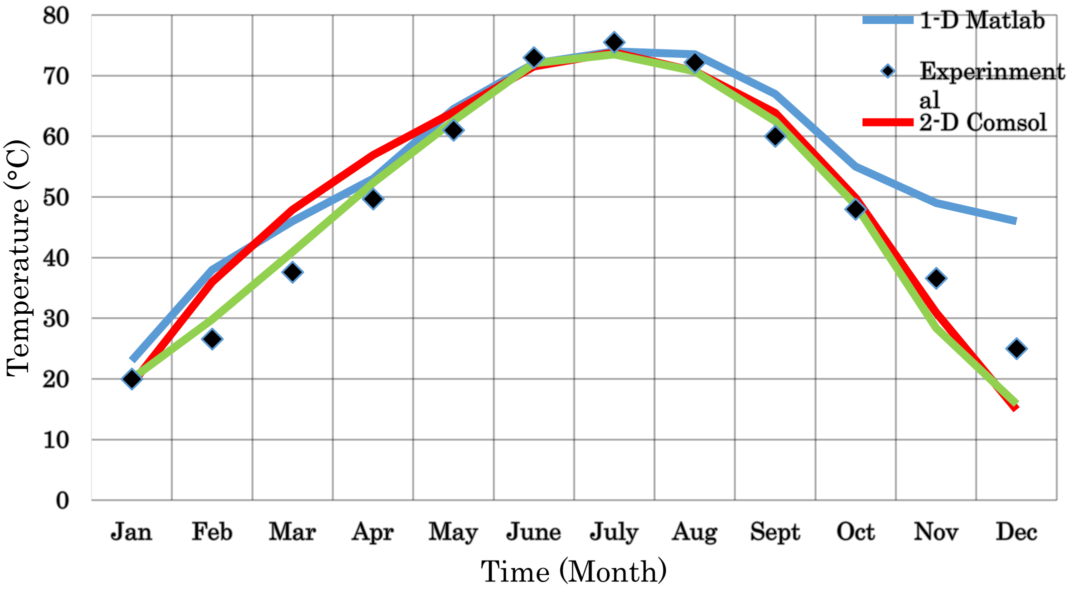

Figure 2: Comparison of 1D (MATLAB) and 2D and 3D (COMSOL) models with Experimental Data, Kuwait SGSP

In Figure 3 a contour plot representing the 3D geometry of the 8m^2 experinmental solar pond located in Kuwait, for a day in the month of June can be seen. The arrows express the direction of the heat loss with the majority being on the surface and a minor percentage from the insulated side walls.

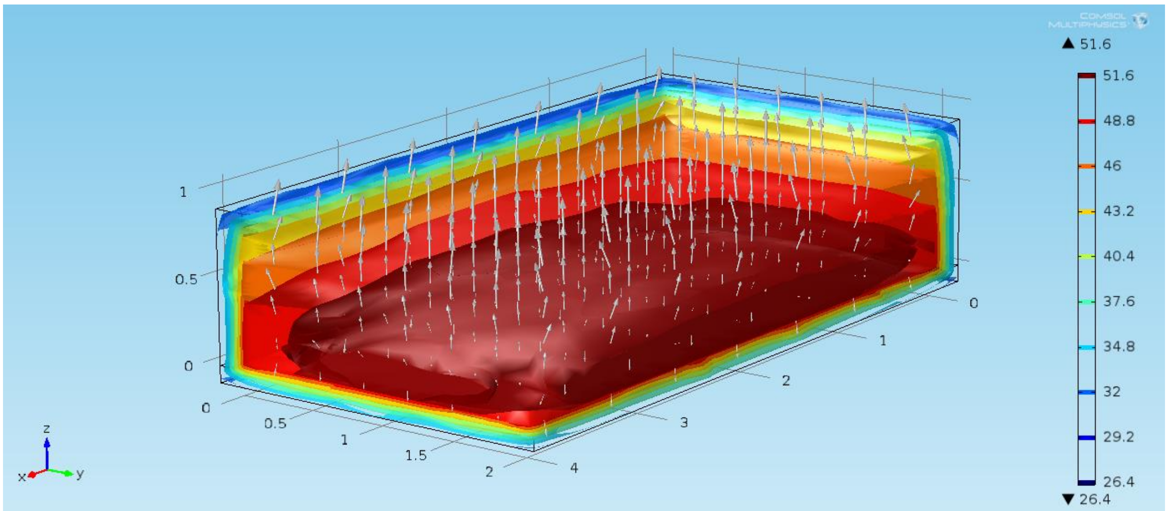

Figure 3: Filled Isothermal Contours, Kuwait Solar Pond, Kuwait SGSP for June (3D Geometry, COMSOL)

3. ADDITTION OF THE NANOPARTICLES

The Al_2O_3 nanoparticles were selected, a common particle that has extended applications in solar collectors. Furthermore, they are the only type of particles that have been used in an experimental study to investigate the performance enhancement of a shallow solar pond Hamdan et al [11]. The properties of these particles are presented in Table 1.

Density	**Specific Heat Capacity**	**Thermal Conductivity**
$3800(kg/m^3)$	$800\ (J/kg\ K)$	$1.2\ (W/kg\ K)$

Table 1: Properties of Al_2O_3 Nanoparticles [26]

The effective density of the nanofluid with respect to the density of the nanoparticle and the density of the base fluid is evaluated as follows [27]:

$$\rho_{nf} = (1-\varphi) * \rho_f + \varphi * \rho_p \tag{5}$$

where φ the volume fraction of nanoparticles, ρ_{nf} the density of nanofluid, ρ_f the density of base fluid, ρ_p the density of the nanoparticle.

The capacitance of the nanofluid is expressed with the formula of Chon et alas [28]:

$$(C_p)_{nf} = \frac{\varphi * \left(\rho * C_p\right)_n + (1-\varphi) * (\rho * C_p)_f}{\varphi * \rho_n + (1-\varphi) * \rho_f} \tag{6}$$

where C_p the specific heat capacity, nf the nanofluid, n the nanoparticle and f the Base fluid

And the thermal conductivity of the nanofluid is expressed as by Kleinstreuer et al [21]:

$$\frac{k_{eff}}{k_{bf}} = 1 + \frac{3 * \left(\frac{k_p}{k_{bf}} - 1\right) * \varphi}{\left(\frac{k_p}{k_{bf}} + 2\right) - \left(\frac{k_p}{k_{bf}} - 1\right) * \varphi} \tag{7}$$

where k_{eff} the effective thermal conductivity of the nanofluid, k_{bf} the thermal conductivity of the base fluid, φ the volume Fraction of nanoparticles in the mixture

Said et al. [29], conducted a time-variant investigation on the optical properties of water based Al_2O_3 nanofluid. They prepared the nanofluids using a two-step method with a follow up of 1h sonication time. They took measurements of the extinction coefficient of the resulting nanofluid, over 6 hours at 1 hour intervals.

In theory the extinction coefficient is the sum of the absorption and scattering coefficient. However, for small spherical particles that are aligned uniformly in a solution, Rayleigh's optical theory explains, that the scattering coefficient is very low and therefore can be neglected. Therefore it can be assumed that the scattering coefficient increases slightly and the majority of the extinction coefficient is attributed to the absorption coefficient [30].

4. APPLICATION OF THE METHODOLOGY - RESULTS

4.1 Introduction

The addition of nanoparticles was simulated for all the validated models. Firstly for the 1-D model and after for the 2-D model. The optimal concentration was identified and was also simulated in the 3-D model.

4.2 1-D Model - MATLAB

The analysis for the 1-D model (Sayer et al, 2016) using the developed code in MATLAB performed for eight concentration of nanofluids, from 0.01% to 0.08% which is the range of practical interest. The results of the analysis are presented in Figure 4, where the computed temperatures at the LCZ are shown on a yearly basis for the various concentrations (e.g volume fractions of nanoparticles in mixture). The respective results for the base case (without nanoparticles) are shown as well.

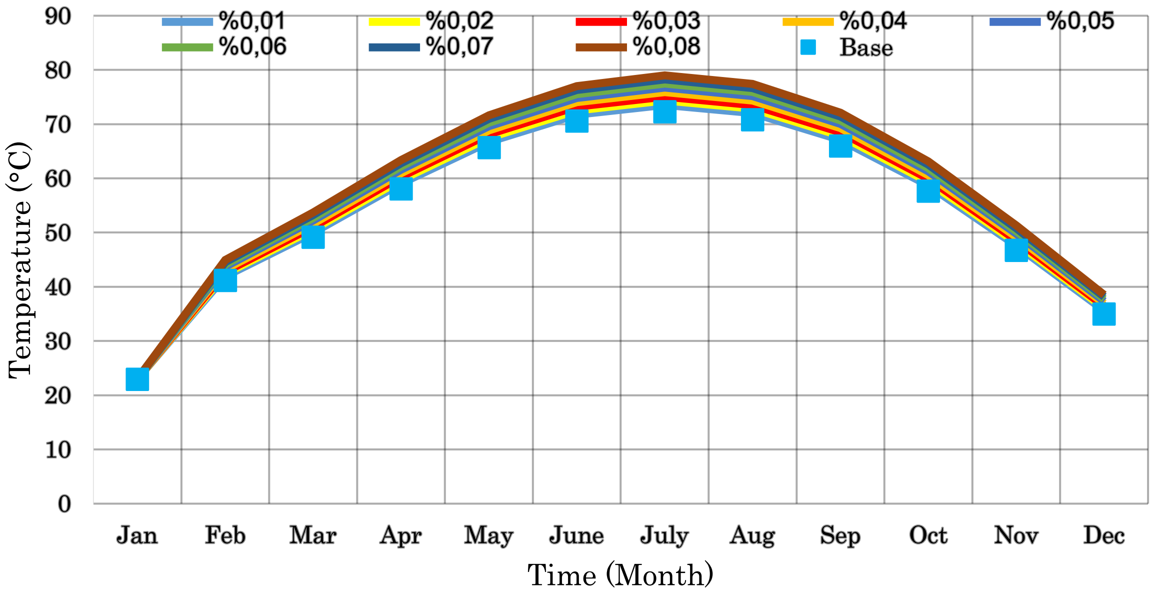

Figure 4: LCZ Temperature for various nanoparticle concentrations, 1-D Model MATLAB, (Kuwait Solar Pond)

It can be seen that the existence of nanofluid has a clear positive effect, and that the temperature increase is analogous to the increase of the nanoparticle concentration. The temperature increase from the base case starts at an average of 1.9°C for a 0.03% and reaches up to an average of 4.86 °C for 0.08%.The maximum improvement is obtained for the 0.08% concentration.

4.3 2-D Model using COMSOL

Following the analysis of the 1-D model the analysis applying the proposed methodology using COMSOL with a 2-D geometry has been performed. Three concentrations of nanofluid have been examined, 0.03%, 0.05% and 0.08%. The intermediate points were not examined as no available data on the optical properties of alumina nanofluid exists for the full range of concentrations.

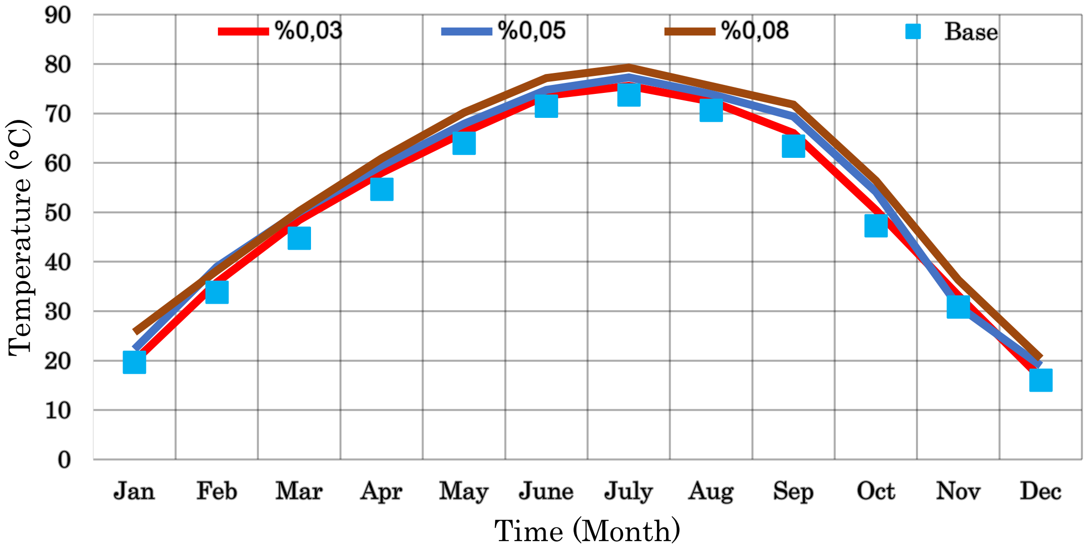

Figure 5: LCZ Temperature for various nanoparticle concentrations, 2D Model (COMSOL), Kuwait Solar Pond

In Figure 5 the differences of the calculated temperatures for concentrations of 0.03%, 0.05% and 0.08% from the base case (without nanofluid) are presented. The model predicts a mean increase in the LCZ of about 2.08ºC, 3,94ºC and 5.93 ºC for concentrations 0.03%, 0.05% and 0.08% respectively. It can be seen that the existence of nanofluid has a clear positive effect, and that the temperature increase is as in the previous cases analogous to the increase of the nanoparticle concentration.

4.4 3D Model using COMSOL

Following the analysis of the 2D model applying the proposed methodology using COMSOL, a 3-D geometry analysis has been performed. The same concentrations as in the 2D case were examined as no data exists for the intermediate points.

In Figure 6 the temperature of the LCZ for the 3 concentrations are presented. It can be seen that, as in the other cases, the existence of nanofluid has a clear positive effect. Furthermore, as seen in the 2D and 1D models the increase in the temperature appears to be analogous to the increase in the concentration. Another notable fact is that the increase in temperature is larger in the summer months than in the other periods. For example for a concentration of 0.08% the increase in the summer is averagely 8.2 ºC, while in the winter months it is only 6,6 ºC. The minimum increase is presented in the winter months for a concentration of 0.03% at 2,6ºC while the maximum for July and a concentration of 0.08% at 9,4 ºC. As in the other cases, the optimal concentration appears to be 0.08% with the 3D model presenting an increased temperature compared to the other two.

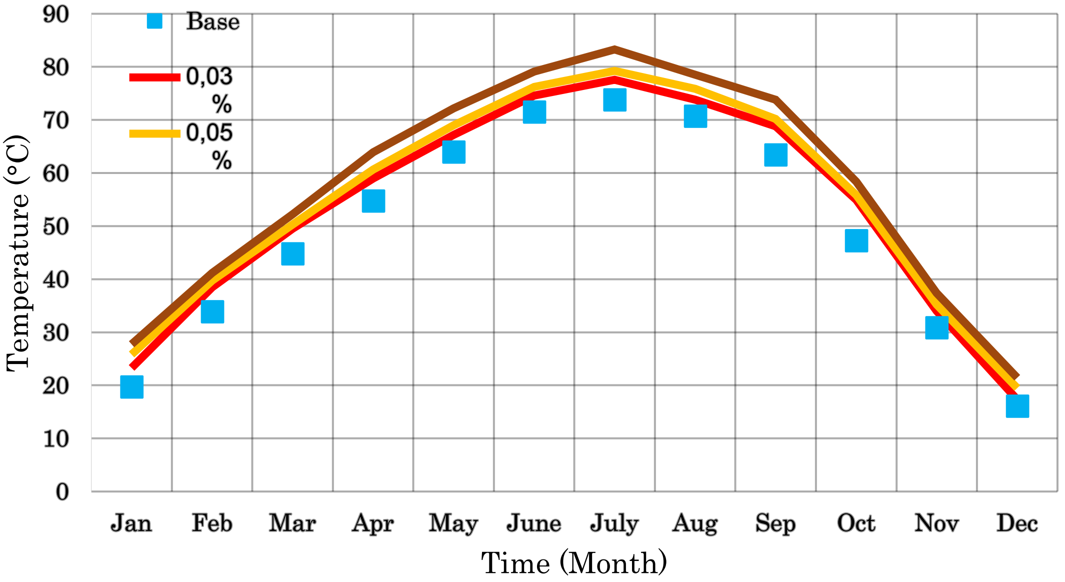

Figure 6: LCZ Temperature for various nanoparticle concentrations, 3D Model (COMSOL), Kuwait Solar Pond

In Figure 7 a snapshot of the side view of the solar pond is presented. The dark red denoting the highest temperatures located at the LCZ, with the blue denoting the lowest temperature, which is a value close to the ambient for the month of July. A noticeable fact is that in this simulation the grey arrows, representing the heat flow outside of the solar pond have a smaller diameter than in the case without nanoparticles. Also, the arrows leaving the dark red area appear to be much smaller and mostly directed to the bottom of the pond. These two observations denote that the thermal properties of the base fluid are enhanced and therefore the conductive heat loss to the fluid above the LCZ has been reduced. The majority of heat loss in the LCZ is now towards the bottom of the tank and not its surface.

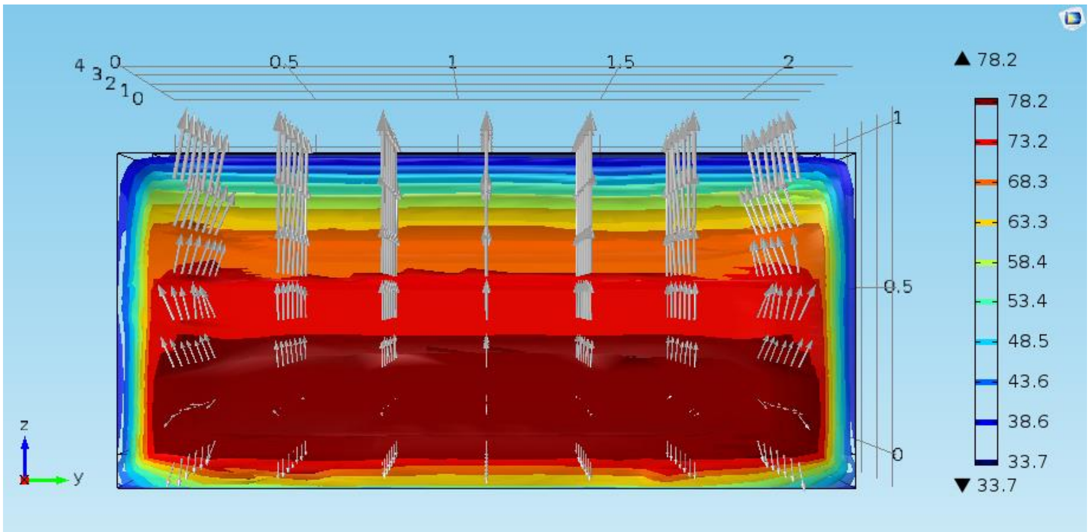

Figure 7: Filled Isothermal Contours, Kuwait Solar Pond, Kuwait SGSP for July (3D Geometry, COMSOL)

5 DISCUSSION-CONCLUSIONS

In the present paper the potential enhancement of the thermal performance of a SGSP using nanofluids in the LCZ was investigated. A numerical analysis was performed using three methods taking into account the change in the thermophysical and optical properties of the base fluid in the solar tank, due to the addition of the nanoparticles.

Due to the nature of used equations in the first method (based on MATLAB) only the thermomechanical properties were changed. In the proposed (and based on COMSOL) methods (2-D and 3-D) both the change of thermophysical and optical properties of the nanofluid were also accounted for. The properties of the nanaofluids have been selected after a thorough literature investigation. The simulations were conducted using the data of an experimental solar pond in Kuwait City, the performance of which was accurately predicted by the model without the existence of the nanoparticles.

The measure of the enhancement of the thermal performance of the SGSP for each case is the difference of the predicted temperatures in the LCZ when nanofluid is used and its corresponding validated base case.

From the above mentioned results it is obvious that the 1-D method of analysis and the 2-D method of analysis give almost the same increase in the temperature of the LCZ. For a concentration of 0.03% the mean value of the increase on a monthly basis is equal to 1.9º C for the 1-D case and 2.1ºC for the 2-D case, whereas for a concentration of 0.08% (the maximum used in practice) the mean increase is 4.86ºC and 5.93º C respectively. In the case of 3-D geometry the increase is much larger. For a concentration of 0,03% there is an increase of 3,9ºC and 5,5 ºC as well as 8,2 ºC for 0,05% and 0.08% respectively.

Since the 3-D model of the thermal performance of the SGSP has been validated using two experimental cases and has been proven that gives more accurate results than the other two, it is logical to accept that its prediction of the thermal performance using nanofluids in the LCZ is more reliable. This increase for the considered range of concentrations 0.03% to 0.08% is of the order of 5ºC to 11ºC respectively. It should be noted that this value is in agreement with the only experimental work existing that of Hamdan et al [11].

As mentioned before these values are theoretical predictions and need for strong experimental verification before to accept the validity of the proposed model for the case of nanofluids.

AKNOWLEDGMENTS

I would like to thank my supervisor Prof. Harvey-Arellano Garcia for his help throughout this project. I would also like to thank Dr. Alasdair Campbell for his advices in the modelling work that was conducted in COMSOL. Furthermore, I would like to thank Dr. A. Sayer for being always available, for answering a lot of questions and problems I had in understanding the physics of the solar ponds and replicating his work in MATLAB.

References

1 Mekhilef, S., Saidur, R. and Safari, A. (2011). A review on solar energy use in industries. *Renewable and Sustainable Energy Reviews*, 15(4), pp.1777-1790.

2 Kanan, S., Dewsbury, J. and Lane-Serff, G. (2015). Simulation of Solar Air-Conditioning System with Salinity Gradient Solar Pond. *Energy Procedia*, 79, pp.746-751.

3 Sing B., (2015), *Power Generation from Solar Pond Using Thermoelectric Generators*, RMIT University PhD, Melbourne

4 Garg, H. (1987). *Advances in solar energy technology*. Dordrecht: D. Reidel Pub. Co.

5 Leblanc, J., Akbarzadeh, A., Andrews, J., Lu, H. and Golding, P. (2011). Heat extraction methods from salinity-gradient solar ponds and introduction of a novel system of heat extraction for improved efficiency. *Solar Energy*, 85(12), pp.3103-3142.

6 Prasher, R., Bhattacharya, P. and Phelan, P. (2005). Thermal Conductivity of Nanoscale Colloidal Solutions (Nanofluids). *Phys. Rev. Lett.*, 94(2).

7 Karunamurthy, K., Murugumohankumar, K. and Suresh, S. (2012). "Use of CuO Nanoparticles for the Improvement of Thermal Conductivity and Performance of Low Temperature Energy Storage System of Solar Pond". *Dig. J. of Nanomaterials and Biostrucutres*, Vol. 7(4), pp.1833-1841

8 Yiamsawas, T., Mahian, O., Dalkilic, A., Kaewnai, S. and Wongwises, S. (2013). Experimental studies on the viscosity of TiO2 and Al2O3 nanoparticles suspended in a mixture of ethylene glycol and water for high temperature applications. *Applied Energy*, 111, pp.40-45.

9 Tyagi, H., Phelan, P. and Prasher, R. (2009). Predicted Efficiency of a Low-Temperature Nanofluid-Based Direct Absorption Solar Collector. *Journal of Solar Energy Engineering*, 131(4), p.041004.

10 Al-Nimr, M. and Al-Dafaie, A. (2014). Using nanofluids in enhancing the performance of a novel two-layer solar pond. *Energy*, 68, pp.318-326.

11 Hamdan, M. and Al-Qudah, L. (2016). "Performance Improvement of Shallow Solar Pond using Nanoparticles."*Int. J. of Thermal Engineering* 11(2), pp.93-98

12 Anagnostopoulos A. (2012). Master Thesis "Modelling of the Thermal Performance of Salinity Gradient Solar Ponds Using COMSOL Multyphysics

13 MATLAB R2013b, The MathWorks, Inc., Natick, Massachusetts, United States.

14 COMSOL Multiphysics 4.0c, COMSOL, Stockholm, Sweden

15 Sayer, A., Al-Hussaini, H. and Campbell, A. (2016). New theoretical modelling of heat transfer in solar ponds. *Solar Energy*, 125, pp.207-218.

16 Wang, Y. and Akbarzadeh, A. (1983). A parametric study on solar ponds. *Solar Energy*, 30(6), pp.555-562.

17 Kishore, V., Joshi, V., 1984. A practical collector efficiency equation for non-convecting solar ponds. *Solar Energy* 33 (5), 391–395.

18 Hull, J. (1980). Computer simulation of solar pond thermal behavior. *Solar Energy,* 25(1), pp.33-40.

19 Swinbank, W. C., (1963), 'Long wave radiation from clear skies', *QJR Meteorol Soc*, 89, pp. 338.

20 Al-Jamal K, Khashan S. Parametric study of a solar pond for northern Jordan. *Energy* 1996;21(10):939

21 Kleinstreuer, C. and Feng, Y. (2011). Experimental and theoretical studies of nanofluid thermal conductivity enhancement: a review. *Nanoscale Res Lett*, 6(1), p.229.

22 Bukata, R. (1995). Optical properties and remote sensing of inland and coastal waters. Boca Raton, Fla.: CRC Press.

23 Rottgers R., Doerferr, R., McKee, D. and Schonfeld, W. (2010). Pure water spectral absorption, scattering, and real part of refractive index model. *Algorithm Technical Basis Document (Draft),* GKKS, STSE, WR D6

24 Röttgers, R., McKee, D. and Utschig, C. (2014). Temperature and salinity correction coefficients for light absorption by water in the visible to infrared spectral region. *Opt. Express,* 22(21), p.25093

25 Ali, H. (1986). Mathematical modelling of salt gradient solar pond performance. *International Journal of Energy Research*, 10(4), pp.377-384.

26 Zhou, S. and Ni, R. (2008). Measurement of the specific heat capacity of water-based Al_2O_3 nanofluid. *Appl. Phys. Lett.*, 92(9), p.093123

27 Vajjha, R. and Das, D. (2012). A review and analysis on influence of temperature and concentration of nanofluids on thermophysical properties, heat transfer and pumping power. *International Journal of Heat and Mass Transfer,* 55(15-16), pp.4063-4078.

28 Chon, C., Kihm, K., Lee, S. and Choi, S. (2005). Empirical correlation finding the role of temperature and particle size for nanofluid (Al_2O_3) thermal conductivity enhancement. *Appl. Phys. Lett.*, 87(15), p.153107.

29 Said, Z., Sajid, M., Alim, M., Saidur, R. and Rahim, N. (2013). Experimental investigation of the thermophysical properties of AL2O3-nanofluid and its effect on a flat plate solar collector.*International Communications in Heat and Mass Transfer*, 48, pp.99-107.

30 Mercatelli, L., Sani, E., Zaccanti, G., Martelli, F., Di Ninni, P., Barison, S., Pagura, C., Agresti, F. and Jafrancesco, D. (2011). Absorption and scattering properties of carbon nanohorn-based nanofluids for direct sunlight absorbers. *Nanoscale Res Lett*, 6(1), p.282.